Direct observation of reptation at polymer interfaces

T. P. Russell*, V. R. Deline*, W. D. Dozier†, G. P. Felcher†, G. Agrawal‡, R. P. Wool‡ & J. W. Mays§

* IBM Research Division, Almaden Research Center, 650 Harry Road, San Jose, California 95120–6099, USA
† Argonne National Laboratory, 9700 South Cass Avenue, Argonne, Illinois 60439, USA
‡ Department of Materials Science and Engineering, University of Illinois at Urbana-Champaign, Urbana, Illinois 61801, USA
§ Department of Chemistry, University of Alabama at Birmingham, Birmingham, Alabama 35294–1240, USA

ALTHOUGH **the diffusion of polymer chains in the liquid state can be described over long distances by classical diffusion laws, chain entanglements make a description of the short-range behaviour more complex. In the standard 'reptation' model[1,2] the polymer chains are considered to move in a curvilinear manner along their own contours, exhibiting snake-like motion through the entangled sea of surrounding molecules. This model successfully explains many observations[3–13], yet no direct evidence for reptative motion has been reported. Here we describe the observation of reptation of molecules across the interface between two types of partially deuterated polystyrene polymers. The time evolution of the hydrogen and deuterium profiles, determined by dynamic secondary-ion mass spectrometry, can be explained only on the basis of a reptation model. Our results demonstrate that, despite being inevitably simplified, the description of polymer diffusion in terms of reptation is essentially correct.**

The reptation model predicts unique interdiffusion profiles at short times[14–16]. Measurements of these profiles in a model-independent manner has, however, not been possible[10,17]. Probably the strongest support for reptation comes from computer simulations[18–21]; but only a few simulations are available on chains of sufficient length to be well entangled.

Consider two layers of polystyrene. Each layer consists of polystyrene chains that have been labelled with deuterium such that ~50% of the protons on the chains have been substituted with deuterium. One layer consists of a DHD-labelled polystyrene triblock copolymer where the lengths of the PSD endblocks are one-half that of the centre PSH block. The second layer is an HDH polystyrene triblock copolymer of equal molecular weight where the labelling has been reversed. HDH and DHD denote the sequencing of the normal polystyrene, PSH, and the perdeuterated polystyrene, PSD, blocks in the molecule. At temperatures above the glass-transition temperature of the polystyrene (~100 °C), the polymer chains begin to interdiffuse across the interface. If the motion of the polymer is the same for each portion of the molecule, the concentration of deuterium across the interface would remain constant. However, if the motion was curvilinear, that is biased towards reptation, this would no longer be true.

The experiment is shown schematically in Fig. 1. Here, the labelled polystyrene molecules are depicted by open and filled circles, where the open circles represent the deuterium-labelled portions of the molecule and the filled circles are the normal (protonated) portions of the chains. Initially, (Fig. 1*a*) the average concentration of the deuteriums-labelled portions of the molecules, ϕ_D, viewed normal to the interface is 0.5. As time proceeds, the molecules diffuse across the interface. If, as shown in Fig. 1*b*, the ends of the chains diffuse first across the interface, followed by the centres of the chains, then for times τ less than the reptation time τ_D (that is, the time it takes for a molecule to diffuse along its own contour), an excess of deuterium on the HDH side (and a depletion on the DHD side) will occur. This is shown in the concentration profile at the right of Fig. 1. As diffusion proceeds, the maximum and minimum in the profile will vanish and a constant concentration profile at 0.5 will again be found.

For these experiments, suitably labelled polystyrene chains must be prepared with well defined molecular weights and narrow molecular-weight distributions. The DHD polymer was synthesized by polymerizing deuterated styrene using a sec-butyl lithium initiator. Normal styrene was then added to the reaction mixture, and polymerization continued, forming a diblock copolymer. The diblock copolymer was then coupled using dichlorodimethylsilane to produce the desired triblock copolymer. This synthesis route ensures that the lengths of the end-labelled portions of the chains are equal. From size-exclusion chromatography the weight-average molecular weight, M_W, of the polymer was found to be 2.25×10^5 with a narrow molecular-weight distribution. An HDH polystyrene with a narrow molecular-weight distribution and $M_W = 2.45 \times 10^5$ was prepared

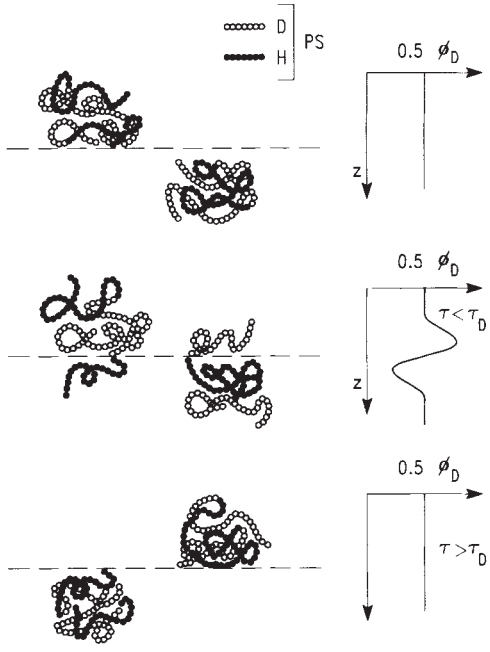

FIG. 1 Diagram of the interface between a bilayer of HDH- and DHD-labelled polystyrene (PS) showing only a few of the polymer chains. The open circles represent the portions of the chains labelled with deuterium and the filled circles are the protonated portions. *a* The initial interface; *b*, the interface after centre-of-mass diffusion over distances less than the radius of gyration; *c* the interface after the molecules have fully diffused across it. The graphs on the right depict the concentration of deuterium as a function of distance across the interface.

in a similar manner. The relative fractions of deuterium labelling were 0.57 and 0.5 for the HDH and DHD polymers, respectively. Films of the DHD polymer, ~100-nm thick, were prepared by spin-coating solutions of the DHD in toluene onto cleaned quartz substrates. These were annealed at 170 °C for 24 hr under vacuum to remove residual solvent and to allow the films to relax. A 100-nm film of the HDH polystyrene was then placed on top of the DHD layer as described elsewhere[10,22]. In the whole process, well tested procedures assured the homogeneity of the films as well as a clean, sharp interface[23].

The profiles of the deuterium and hydrogen across the interface were determined by dynamic secondary-ion mass spectrometry (DSIMS) with a depth resolution of 5 nm. Using a Perkin Elmer 6300 secondary-ion mass spectrometer, a 2-keV O_2^+ beam (200 nA directed 60° from the surface normal and rastered over an area of 500 μm × 500 μm) was used to sputter the polystyrene. Secondary ions of H^- and D^- were collected from the central 9% of the rastered area. A low-energy electron beam was used to compensate the positive surface charging that occurred. The depths of the sputtered craters were measured to convert the sputtering time to distance. The initial DSIMS profiles showed a difference between the H and D content in the HDH and DHD layers. These profiles were used as a baseline and subtracted from the remaining H and D depth profiles to yield the H and D excess. (For clarity, only the excess of D, normalized by the initial D signal in the DHD layer, is reported here.) The interdiffusion of the bilayers was performed by heating the samples in vacuum to 118 °C for the desired time, followed by quenching to room temperature. Figure 2*a* and *b* shows the excess of D as a function of depth for the different annealing times.

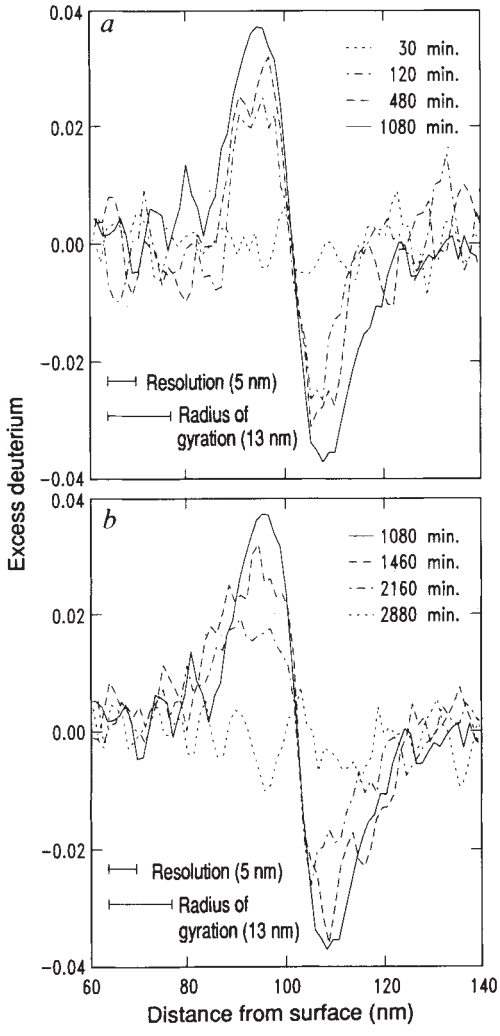

FIG. 2 Excess deuterium determined by DSIMS as a function of distance for the HDH- and DHD- polystyrene bilayers after interdiffusion at 118 °C for the times specified. In *a* the amplitude of the excess deuterium increases with time, whereas in *b* the excess deuterium decreases with time. *a*, ···, 30 min; ·−·, 120 min; −−, 480 min; —, 1,080 min. *b*, —, 1,080 min; −−, 1,460 min; ·−·, 2,160 min; ····, 2,880 min.

The rise and decay of the maximum and minimum in the profiles are clearly seen, which, taking into account the instrumental resolution, follow a behaviour characteristic of reptation. The results show that distances over which the maximum and minimum extend are comparable to the radius of gyration, R_g, of the polystyrene (indicated in Fig. 2). These results were checked against possible artefacts. First, we note that subtracting the initial profile from subsequent profiles is not correct. By simple fickian diffusion the interface will broaden to give a similar effect. However, the amplitudes of the signal from such an effect are too small to be observable over the timescale studied. Also, the maximum and minimum would be seen on the opposite sides of the interface as experimentally observed. Second, surface-segregation effects were examined on separate films and found to be of no consequence. The results were independent of the sequencing of the layers. Finally the experiment was designed to minimize the excess (non-ideal) free energy of mixing between the HDH and DHD layers, which acts to retard the diffusion.

These results demonstrate that the diffusion of polymer chains across the interface must occur by some kind of reptative process. Isotropic fluctuations of chain segments across the interface are not observable in this experiment because of the nature of the labelling. In fact, nearly 120 min (slightly less than the Rouse relaxation time of the entire chain, that is, the relaxation time of internal modes in the chain) were required before any excess was observable. The spatial separation of the maximum and minimum in the profile of D excess was time-invariant but the breadth of the signal increased with time. The amplitude of the excess reached a maximum at ~1,080 min and had vanished by 2,880 min, which corresponds well to the calculated reptation time τ_D for these polymers at 118 °C is ~2,200 min. Thus, it has been shown that the chain ends lead the chain centres over a time during which the whole chain has diffused a distance equal to R_g. This is curvilinear or reptative motion. Our unpublished simulations based on pure reptation yield results in agreement with the observations shown here. Similar studies are being done on different molecular-weight pairs of polystyrene, both above and below the entanglement molecular weight ($\sim 2 \times 10^4$). Experiments are also in progress using other techniques with better spatial resolution to provide a definitive set of data to test the details of theoretical predictions and computer simulations[24]. □

Received 14 April; accepted 23 July 1993.

1. de Gennes, P.-G. J. *Chem. Phys.* **55,** 572–579 (1971).
2. Doi, M., Edwards, S. J. *J. chem. Soc., Faraday Trans.* 2 **74,** 1789–1801, 1802–1817, 1818–1832 (1978).
3. Klein, J. *Nature* **271,** 143–145 (1978).
4. Green, P. F., Mills, P. J., Palmstrom, C., Mayer, J. W. & Kramer, F. J. *Phys. Rev. Lett.* **53,** 2145–2148 (1984).
5. Richter, D. *Phys. Rev. Lett.* **64,** 1389–1392 (1990).
6. Butera, R. *et al. Phys. Rev. Lett.* **66,** 2088–2091 (1991).
7. Tassin, J. F., Monnerie, L. & Fetters, L. J. *Macromolecules* **21,** 2404–2412 (1988).
8. Ylitalo, C. M., Fuller, G. G., Abetz, V., Stadtler, R. & Pearson, D. S. *Rheol. Acta* **29,** 543–555 (1990).
9. Lee, A. & Wool, R. P. *Macromolecules* **19,** 1063–1068 (1986); **20,** 1924–1927 (1987).
10. Karim, A. *thesis, Northwestern Univ.* (1990).
11. Whitlow, S. J. & Wool, R. P. *Macromolecules* **24,** 5926–5938 (1991).
12. Osaki, K. *et al. Macromolecules* **22,** 2457–2460 (1989).
13. Wool, R. P. *Structure and Strength of Polymer Interfaces* (Hanser, New York (1993).
14. Brochard-Wyart, F. & de Gennes, P. G. *Physico-Chemical Hydrodyn.* **4,** 313–322 (1983).
15. Tirrell, M., Adolf, D. & Prager, S. *Springer Lecture Notes in Appl. Math.* **163,** 37–45 (Springer, Heidelberg, 1984).
16. Harden, J. L. *J. Phys. Paris,* **51,** 1777–1784 (1990).

17. Reiter, G. & Steiner, U. *J. Phys. II* **1,** 659–671 (1991).
18. Kremer, K. & Grest, G. S. *J. chem. Phys.* **92,** 5057–5086 (1991).
19. Paul, W., Binder, K., Heermann, D. W. & Kremer, K. *J. Phys. II* **1,** 37–60 (1991).
20. Paul, W., Binder, K., Heermann, D. W. & Kremer, K. *J. chem. Phys.* **95,** 7726–7740 (1991).
21. Crabb, C. C. & Kovac, J. *Macromolecules* **18,** 1430–1435 (1985).
22. Russell, T. P., Karim, A., Mansour, A. & Felcher, G. P. *Macromolecules* **21,** 1890–1893 (1988).
23. Karim, A., Mansour, A., Felcher, G. P. & Russell, T. P. *Mater. Res. Soc. Symp.* **171,** 329–333 (Mater. Res. Soc., Pittsburgh, 1990).
24. Agrawal, G. *et al. Macromolecules* (submitted).

Dynamic enhancement of cation migration in a Zintl alloy by polyanion rotation

Marie-Louise Saboungi*, Jeffrey Fortner*, W. Spencer Howells† & David Long Price*

* Argonne National Laboratory, Argonne, Illinois 60439, USA
† Rutherford–Appleton Laboratory, Chilton, Oxon OX11 0QX, UK

ZINTL alloys are compounds of an alkali metal A with a polyvalent metal M in which transfer of an electron from A to M leads to bonding behaviour in the M^- ions typical of elements one column to the right in the Periodic Table. For example, ASn and APb contain tetrahedral M_4^{4-} polyanions in both the crystalline and liquid phases[1] whereas AAl alloys crystallize in tetrahedrally bonded networks typical of Group IV elements[2]. These bonding patterns also determine the character of the disorder in the solid at high temperature. We have recently identified a plastic crystal phase in CsPb just below the melting point, in which the Pb_4^{4-} polyanions undergo jump reorientations[3]; LiAl, in contrast, is metallic, with mobile Li^+ ions[4]. Here we report unusual disordering behaviour in the Zintl alloy NaSn, in which both types of dynamic disorder appear: rapid reorientations of the Sn_4^{4-} polyanions enhance jump migration of the Na^+ cations by means of a 'paddle-wheel' effect. The two types of disorder are strongly coupled, so that only one disordering transition takes place as the melting point is approached.

NaSn is an alloy well known since 1928, when Hume-Rothery[5] made a careful study of its phase diagram. Although Hume-Rothery's diagram has since been modified in some details[6], his general scheme has been validated by subsequent work; for example, his values for the transition and melting temperatures of the compound NaSn agree with our recent calorimetry measurements[7] to within 1–2 °C. An interesting feature of the phase diagram is a transition (over the entire composition range of the solid) at 483 °C, ~95 °C below the congruent melting point. Hume-Rothery referred to this simply as a "polymorphic phase transformation in the solid", and to our knowledge it has not been explored since.

The transition is dramatically reflected in both thermodynamic properties. Figure 1*a* shows the enthalpy of NaSn derived from our calorimetric measurement[7]. The entropy change at the transition, $T_1 = 484$ °C, is $\Delta S_1 = 4.95$ J mol^{-1} K^{-1}, comparable to the entropy of melting, $\Delta S_m = 8.48$ J mol^{-1} K^{-1}. The electrical conductivity measured for NaSn as a function of temperature[8] is shown in Fig. 1*b*, and shows a sharp drop at the transition followed by a rapid rise towards the melting point. This general behaviour is qualitatively consistent with current understanding about the electronic structure of NaSn: band-structure calculations[9,10] show the low-temperature solid phase to be a narrow-gap semiconductor with a direct band gap of ~0.3 eV.

The low-temperature (β) phase has the NaPb crystal structure found in all the ASn and APb alloys (A = Na, . . . Cs)[11]. Nearly perfectly tetrahedral Sn_4^{4-} anions lie on a body-centred tetragonal lattice separated by Na^+ cations on two types of site, namely Na(1) sites forming tetrahedra concentric with, and oppositely directed to, the Sn_4^{4-} tetrahedra and Na(2) sites forming squares in the (a–b) plane, also concentric with the Sn_4^{4-} tetrahedra. All Na sites can be considered to be shared between two Sn_4^{4-} tetrahedra. No crystallographic data are available, to our knowledge, for the high-temperature (α) phase. Neutron diffraction studies of the liquid[12] indicate that the Sn_4^{4-} polyanions survive into the melt, although the 'first sharp diffraction peak' characteristic of intermediate-range order, which in this case would result from a random packing of the tetrahedra, is not as pronounced as in other ASn and APb alloys apart from NaPb (ref. 1).

The relatively large entropy change of the β–α transition suggested that the α-phase might be dynamically disordered. To investigate this possibility, quasielastic neutron scattering (QENS) measurements were carried out on the IRIS spectrometer at the ISIS pulsed spallation source[13]. The IRIS spectrometer incorporates a detector at high angle with which a diffraction pattern can be collected, making it possible to monitor closely the changes in state with temperature and also to derive structural information about the current phase of the sample. The diffraction patterns of the β-phase were consistent with the reported structure[11], and no additional Bragg peaks were observed. At the β–α transition, the Bragg peaks around a scattering vector $Q \sim 1$ Å^{-1} were replaced by a set of lower-symmetry peaks, consistent with a triclinic structure. (D.L.P., M.L.S. and J. W. Richardson, unpublished data.) At higher Q the Bragg peaks were greatly attenuated and replaced by diffuse scattering, peaking around $Q \sim 2$ Å^{-1}, as in the liquid. All the Bragg peaks disappeared on melting and the remaining diffuse scattering was consistent with the reported liquid structure[12].

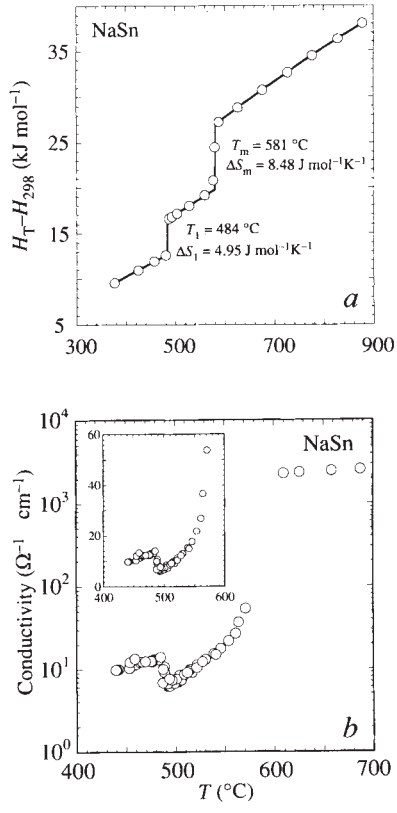

FIG. 1 *a*, Enthalpy, and *b*, electrical conductivity of NaSn as a function of temperature. The inset in *b*, shows the behaviour at the transition on an expanded scale (units on axes same as main graphs).